

Thermal Decomposition of Prussian Blue Analogues of the Type $\text{Fe}[\text{Fe}(\text{CN})_5\text{NO}]$

Hiddenari Inoue^a, Shuichi Narino^a, Naoki Yoshioka^a, and Ekkehard Fluck^b

^a Department of Applied Chemistry, Keio University,
3-14-1 Hiyoshi, Kohoku-ku, Yokohama 223-8522, Japan

^b Max-Planck-Haus, Berliner Strasse 10, D-69120 Heidelberg, Germany

Reprint requests to Prof. Dr. Dr. h. c. E. Fluck. Fax: +49 (0)6221 486-385

Z. Naturforsch. **55 b**, 685–690 (2000); received April 5, 2000

Prussian Blue Analogues, Mixed-Valence State, Thermal Decomposition

The structure and properties of the thermal decomposition products of $\text{Fe}[\text{Fe}(\text{CN})_5\text{NO}] \cdot x\text{H}_2\text{O}$ ($x = 5\sim 6$) have been studied by Mössbauer and FT-IR spectroscopy, X-ray diffraction, and conductivity measurements. The valence state and coordination environment of the iron ions change dramatically when the nitrosyl ligand is eliminated by heat-treatment under vacuum at 200 °C. The dark blue product obtained by heat-treatment under vacuum at 250 °C is characteristic of the mixed-valence state in Prussian blue analogues. The electrical conductivity of the dark blue product is higher by a factor of 10^3 than that of the starting material because of the mixed-valence state between $\text{Fe(III)}[\text{Fe(II)}(\text{CN})_5]$ and $\text{Fe(II)}[\text{Fe(III)}(\text{CN})_5]$. Heat-treatment under vacuum at 350 °C yields a new product $\text{Fe(II)}[\text{Fe(II)}(\text{CN})_4]$ the crystal structure of which is different from that of the starting material. The electrical conductivity of the decomposition product obtained at 350 °C is about 10^3 times higher than that of the starting material.

Introduction

Prussian blue and its analogues have attracted a great deal of attention because of their importance in functional pigments, electrochromic materials and semiconductors. Their interesting properties are associated with the mixed-valence state. Of the synthetic methods of these functional materials, heat-treatment under vacuum, *i. e.* vacuum pyrolysis, has been a useful means to produce the mixed-valence states [1]. Although the thermal decomposition of Prussian blue and its analogues has been reported in previous papers [2 - 3], little attention has been focused on analogues of the type $\text{Fe}[\text{Fe}(\text{CN})_5\text{NO}]$. Surprisingly, Prussian blue analogues of the type $\text{M}[\text{Fe}(\text{CN})_5\text{NO}] \cdot x\text{H}_2\text{O}$ ($\text{M} = \text{Mn}, \text{Fe}, \text{Co}, \text{Ni}, \text{Cu}$ and Zn) have been investigated by a variety of spectroscopic methods, *e. g.* electronic absorption [4], infrared absorption [5, 6], Mössbauer [7, 8] and X-ray photoelectron spectroscopy [9]. However, the thermal decomposition of $\text{M}[\text{Fe}(\text{CN})_5\text{NO}] \cdot x\text{H}_2\text{O}$ has received less attention, although a few Prussian blue analogues have been extensively studied [10]. In the present work we have attempted to produce a new type of mixed-valence state or electronic state in macromolecular complexes by heat-treatment of

$\text{Fe}[\text{Fe}(\text{CN})_5\text{NO}] \cdot x\text{H}_2\text{O}$ under vacuum. It has been demonstrated that the physical properties such as electrical conductivity are dramatically improved by this treatment.

Experimental

Materials

Sodium pentacyanonitrosylferrate(II) dihydrate was obtained from Wako Pure Chemical Ind., iron(II) sulfate heptahydrate was purchased from Kanto Chemicals Co. and used without further purification. All solvents used were of reagent grade and used as received. $\text{Fe}[\text{Fe}(\text{CN})_5\text{NO}] \cdot x\text{H}_2\text{O}$ ($x = 5\sim 6$) was prepared as follows. A 0.02 M aqueous solution (100 cm³) of $\text{FeSO}_4 \cdot 7\text{H}_2\text{O}$ was added to a 0.02 M aqueous solution (100 cm³) of $\text{Na}_2[\text{Fe}(\text{CN})_5\text{NO}] \cdot 2\text{H}_2\text{O}$ with stirring. After adding 200 cm³ of acetone the mixed solution was allowed to stand overnight. The precipitates obtained were collected by filtration, washed with distilled water till sulfate ions could not be detected in the filtrate, and finally washed with acetone and dried in air for a week.

Heat-treatment under vacuum

The sample was pre-dried in vacuo at 120 °C for 8 h to remove water. The sample was then heated under vacuum in a quartz tube at different temperatures (200 ~ 350 °C)

for 24 h and subsequently quenched to liquid nitrogen temperature in a Dewar vessel.

Instruments

The infrared spectra were obtained with a BIO-RAD FTS-65 infrared spectrometer on KBr pellets and Nujol mulls. The X-ray diffraction powder patterns were taken at room temperature with a Rigaku-Denki Geigerflex RAD-C X-ray diffractometer using graphite-monochromated Cu-K α radiation ($\lambda = 0.1542$ nm). Thermogravimetric analyses (TG) and differential thermal analyses (DTA) were carried out simultaneously by using a Seiko TG/DTA 320 thermal analyzer. About 40 mg of powdered samples were heated at the constant rate of 5°Cmin^{-1} in an atmosphere of argon. The DTA curves were also recorded at the heating rate of 5°Cmin^{-1} with α -alumina as reference material in an atmosphere of argon. The Mössbauer spectra were measured by a Wissel constant-acceleration transducer coupled with an ORTEC 5500 multichannel analyzer. A 370 MBq ^{57}Co source in rhodium was purchased from The Radiochemical Centre, Amersham, England. The spectra obtained at 293 K were fitted to Lorentzian curves using an iterative least-squares computer program. The isomer shifts were referred to the symmetry center of the sextet of natural iron foil kept at 293 K. The electrical conductivity of the heat-treated samples was measured with a Takeda-Riken TR-8651 electrometer by the usual current-voltage method. The details of the conductivity measurements were already described in [11].

Results and Discussion

Thermal analysis

The water in $\text{Fe}[\text{Fe}(\text{CN})_5\text{NO}] \cdot x\text{H}_2\text{O}$ can be removed upon heating under vacuum without any change in the three-dimensional framework of $\text{Fe}[\text{Fe}(\text{CN})_5\text{NO}]$. The process is reversible at temperatures lower than 120°C . As Fig. 1 shows, the thermogravimetric (TG) and differential thermal analysis (DTA) indicate that $\text{Fe}[\text{Fe}(\text{CN})_5\text{NO}] \cdot x\text{H}_2\text{O}$ begins to lose water around 50°C and is endothermically dehydrated at 144°C . The water content calculated from the weight loss of the TG curve corresponds to $x = 5.6$. The water content in $\text{Fe}[\text{Fe}(\text{CN})_5\text{NO}] \cdot x\text{H}_2\text{O}$ varied in the range from 5 to 6 depending on the atmosphere to which the compound is exposed.

After the endothermic dehydration, $\text{Fe}[\text{Fe}(\text{CN})_5\text{NO}]$ decomposes gradually between

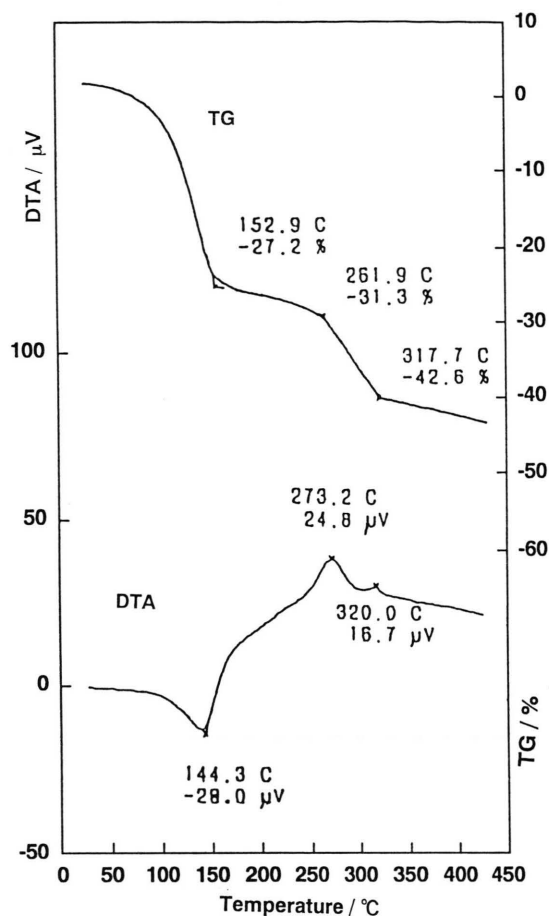


Fig. 1. TG and DTA curves of $\text{Fe}[\text{Fe}(\text{CN})_5\text{NO}] \cdot x\text{H}_2\text{O}$.

153 and 262°C with the evolution of nitrogen oxide and/or cyanogen gas. This decomposition process is slightly exothermic in the DTA curve, but not explicitly observed in the TG curve. Presumably the loss rate of cyanogen and nitrogen monoxide is very slow [11]. Further heating causes a sharp exothermic decomposition at 273°C and leads to the formation of $\text{Fe}[\text{Fe}(\text{CN})_4]$, followed by an exothermic decomposition at 320°C ascribed to the structural rearrangement of the cyano ligands. The gaseous products released during the pyrolysis at 250°C were analyzed earlier by conventional spectrophotometric methods [12].

Structural change with thermal decomposition

The starting material $\text{Fe}[\text{Fe}(\text{CN})_5\text{NO}] \cdot x\text{H}_2\text{O}$ ($x = 5\sim 6$) crystallizes in space group $Fm\bar{3}m$, $a = 1042$ pm, $Z = 4$ [4, 7]. The face-centered cubic

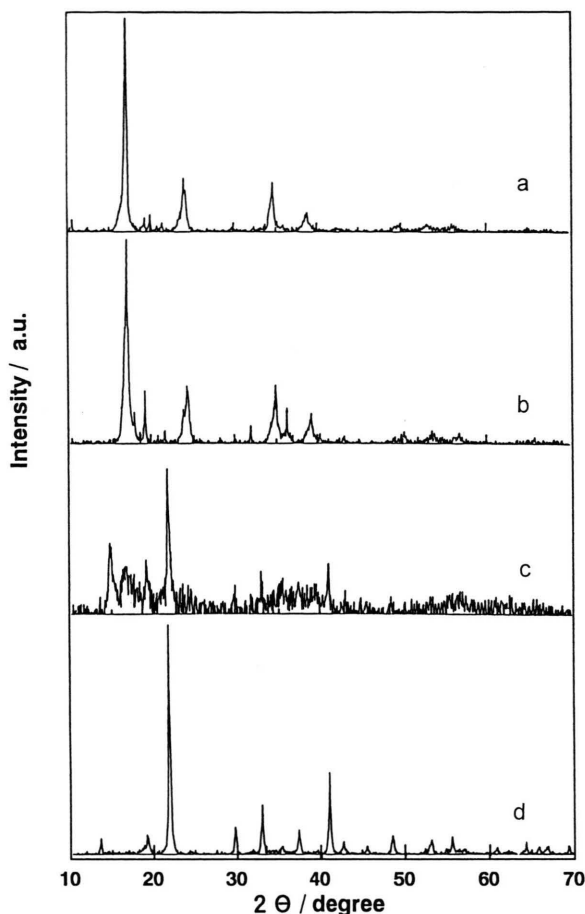


Fig. 2. X-ray diffraction powder patterns of starting material (a) and the samples heated at 200 °C (b), at 300 °C (c) and at 350 °C (d).

unit cell forms the three-dimensional framework $\text{Fe}^{\text{II}}\text{--C}\equiv\text{N--Fe}^{\text{II}}$ in which $\text{Fe}[\text{Fe}(\text{CN})_5\text{NO}] \cdot x\text{H}_2\text{O}$ ($x = 5\sim 6$) consists of the high-spin Fe^{II} coordinated by the nitrogen ends of the cyano ligands and the oxygen end of the nitrosyl ligand and the low-spin Fe^{II} coordinated by the carbon ends of the cyano ligands and the nitrogen end of the nitrosyl ligand. As Fig. 2 shows, the X-ray powder diffraction pattern of the sample heated under vacuum at 200 °C for 24 h is much the same as that of the starting material, suggesting that the three-dimensional framework characteristic of Prussian blue analogues is still maintained although a few peaks begin to appear in the heat-treated sample. At this stage the color of the product is quite similar to that of Prussian blue. After 24 h of heating under vacuum at

Table 1. IR data of heat-treated samples in the CN and NO stretching region.

Sample	Heat-treatment temp. (°C)	Assignment ν_{CN} (cm^{-1})	ν_{NO} (cm^{-1})
a	not treated ^a	2184(vs) ^b	1934(vs)
b	200	2186(w), 2076(vs)	1949(w)
c	300	2076(vs)	—
d	350	2076(sh), 2033(vs)	—

^a Starting material; ^b vs = very strong; w = weak; sh = shoulder.

300 °C, the X-ray diffraction peaks (Fig. 2) of the starting material disappear. The sample heated under vacuum at 350 °C for 24 h exhibits a new well-resolved X-ray diffraction pattern, indicating that a structural rearrangement of the cyano ligands or a crystallization of amorphous intermediates occurs between 300 and 350 °C. This is supported by the fact that an exothermic peak without weight loss is observed at 320 °C in the DTA curve (*cf.* Fig. 1). However, many efforts failed to index the diffraction peaks to a plausible crystal system probably due to the presence of impurities.

The IR spectral data of the solid residue obtained by heating under vacuum at 200, 300, and 350 °C are listed together with those of the starting material in Table 1. Besides the CN stretching band at 2184 cm^{-1} of the starting material, a new broad CN stretching band appears around 2076 cm^{-1} in the sample treated under vacuum at 200 °C. The NO stretching band observed around 1934 cm^{-1} disappears almost completely after heating the sample to 250 °C for 24 h. The intermediate produced at 300 °C under vacuum exhibited $\nu(\text{C}\equiv\text{N})$ around 2076 cm^{-1} which is shifted to lower frequencies by about 108 cm^{-1} as compared with the starting material and similar to that of Prussian blue, *i. e.* iron(III) hexacyanoferrate(II). This large shift is comparable to that observed on going from ferricyanide to ferrocyanide [13], suggesting that upon heating above 250 °C the reduction of the central iron(III) ion to the iron(II) ion occurs with loss of cyanogen gas. The $\nu(\text{CN})$ of the sample heated to 350 °C appeared at 2033 cm^{-1} with a shoulder around 2076 cm^{-1} , dramatically shifted to lower frequencies by about 43 cm^{-1} compared with that observed for the sample heated to 300 °C. This large shift in the CN stretching band is consistent with the conclusion drawn from the X-ray powder diffraction of the ther-

Sample	Heat-treatment temp. (°C)	Mössbauer parameter δ (mms ⁻¹)	Mössbauer parameter ΔE_Q (mms ⁻¹)	Assignment
a	not treated ^a	-0.32	1.89	Fe(CN) ₅ NO ²⁻ (low-spin)
		1.11	1.49	Fe ²⁺ (high-spin)
b	200	-0.33	1.92	Fe(CN) ₅ NO ²⁻ (low-spin)
		1.10	1.51	Fe ²⁺ (high-spin)
		-0.19	–	Fe(CN) ₅ ³⁻ (low-spin)
		0.36	0.68	Fe ³⁺ (high-spin)
c	300	-0.14	–	Fe(CN) ₅ ³⁻ (low-spin)
		0.31	0.55	Fe ³⁺ (high-spin)
		1.29	0.90	Fe ²⁺ (high-spin)
d	350	-0.14	–	Fe(CN) ₄ ²⁻ (low-spin)
		1.07	–	Fe ²⁺ (high-spin)

Table 2. Mössbauer parameters obtained at 293 K and peak assignment.

^a Starting material.

mal decomposition product, indicating a structural rearrangement or a crystallization of amorphous intermediates between 300 and 350 °C.

Electronic structure of thermal decomposition products

The ⁵⁷Fe Mössbauer spectra of the samples are shown in Fig. 3 together with that of the starting material. The Mössbauer parameters obtained at 293 °C are listed in Table 2. The Mössbauer spectrum of the starting material Fe[Fe(CN)₅NO]·xH₂O consists of a pair of quadrupole doublets. One is assigned to the low-spin iron(II) ion of the Fe(CN)₅NO²⁻ moiety and the other is attributed to the high-spin iron(II) ion [14]. The sample heated to 200 °C for 24 h exhibits a singlet and a quadrupole doublet other than a pair of quadrupole doublets originating from the starting material. The new doublet is characteristic of high-spin Fe(III) complexes, while the new singlet is typical of low-spin Fe(II) complexes. These peaks become predominant in the sample heated to 250 °C. Clearly, at 270 °C almost all of the starting material is converted to a new material tentatively assigned to Fe[Fe(CN)₅]. This mixed-valence compound is probably the reason why the area ratio of the singlet absorption peak to the quadrupole doublet peak is not unity (*cf.* Fig. 3 (b) and (c)).

In the Mössbauer spectrum of the sample heated to 300 °C, a new quadrupole doublet with $\delta = 1.29$ mms⁻¹ and $\Delta E_Q = 0.90$ mms⁻¹ appears. This doublet is assigned to a high-spin iron(II) species which is produced by evolution of cyanogen gas from Fe[Fe(CN)₅]. It is noteworthy that the combination of the singlet and the quadrupole doublet is quite similar to that observed for Prussian blue. As Fig. 3(d) shows, the sample heated to 350 °C

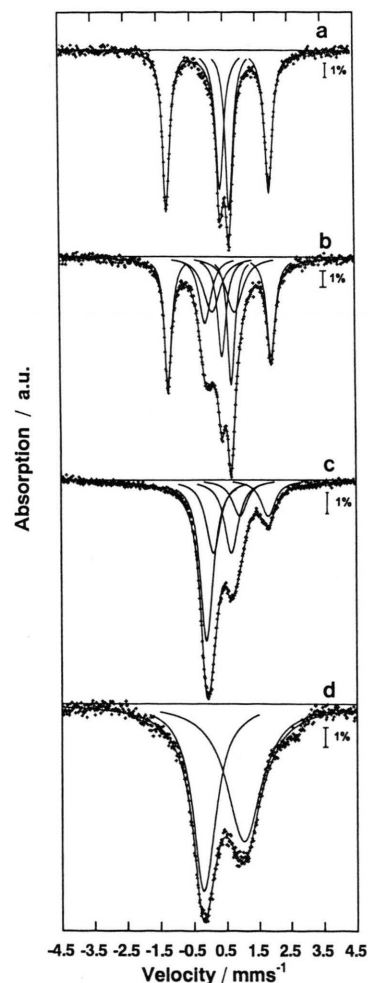


Fig. 3. ⁵⁷Fe Mössbauer spectra of starting material (a) and the samples heated at 200 °C (b), at 300 °C (c) and at 350 °C (d).

for 24 h exhibits several singlets which can be assigned to the low-spin and high-spin iron(II) species

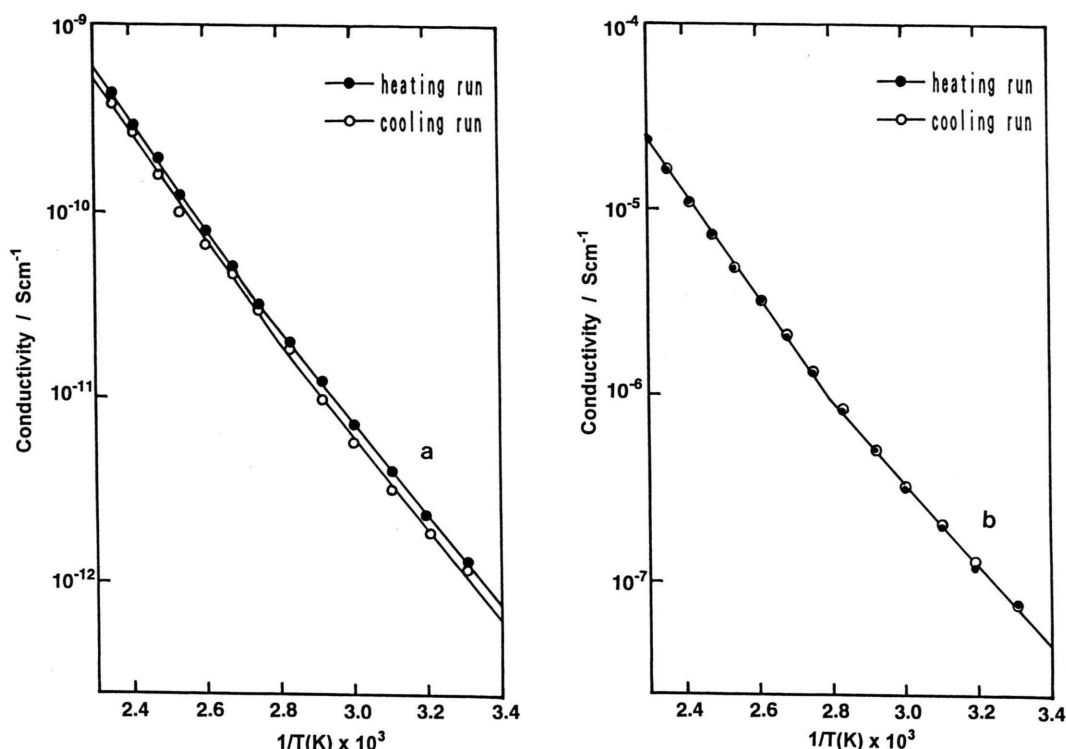


Fig. 4. Plots of the logarithm of electrical conductivity versus $1/T$ for starting material (a) and the sample heated at 300 °C (b).

probably corresponding to a product of the formula $\text{Fe(II)[Fe(II)(CN)}_4]$.

Electrical conductivity of thermal decomposition products

Plots of the logarithm of electrical conductivity σ versus $1/T$ are shown for the starting material and the sample heat-treated at 300 °C in Fig. 4. As expected, the temperature-dependence of the conductivity is characteristic of semiconductors and obeys the law $\sigma = \sigma_0 \exp(-E_a/kT)$, where σ_0 is a constant, E_a the activation energy of electrical conduction, k the Boltzmann constant, respectively. The specific conductivity of the starting material $\text{Fe}[\text{Fe}(\text{CN})_5\text{NO}] \cdot x\text{H}_2\text{O}$ is small compared to that of Prussian blue $\text{Fe}_4[\text{Fe}(\text{CN})_6]_3 \cdot x\text{H}_2\text{O}$ [10,11]. This is probably due to the absence of the mixed-valence state as in Prussian blue. The conductivity of the sample heated at 200 °C is significantly improved and further increased for the sample heated at 300 °C. This conductivity does not change much

Table 3. Specific conductivity and activation energy of heat-treated samples.

Sample	Heat-treatment temp. (°C)	Specific conductivity at 293 K (Scm^{-1})	Activation energy (eV)
a	not treated ^a	5.8×10^{-13}	0.51 (0.59) ^b
b	200	1.1×10^{-9}	0.49 (0.59)
c	300	4.1×10^{-8}	0.44 (0.57)
d	350	8.5×10^{-8}	0.38 (0.45)

^a Starting material; ^b activation energy in the higher temperature region.

after heat-treatment at 350 °C for 24 h, even though the compound turns crystalline in this temperature range.

The activation energy of electrical conduction was calculated from the slope of the $\log \sigma$ versus $1/T$ plots and listed together with the specific conductivity in Table 3. It is interesting to note that except for the starting material the activation energies in the impurity and intrinsic regions decrease as the temperature of the heat-treatment is raised. The lowering of the activation energies is ascribed to the

mixed-valence state created by the heat-treatment of $\text{Fe}[\text{Fe}(\text{CN})_5\text{NO}] \cdot x\text{H}_2\text{O}$. The conduction mechanism in Prussian blue and its analogs has been described in terms of the band model [10] and elec-

tron hopping [11]. These two models might be also applicable to the interpretation of the conduction mechanism in the thermal decomposition products of $\text{Fe}[\text{Fe}(\text{CN})_5\text{NO}] \cdot x\text{H}_2\text{O}$.

-
- [1] J. G. Cosgrove, R. L. Collins, D. S. Murty, *J. Am. Chem. Soc.* **95**, 1083 (1973).
- [2] B. Mohai, A. Horváth, P. E. Honti, *J. Thermal. Anal.* **31**, 157 (1986).
- [3] H. Inoue, T. Nakazawa, T. Mitsuhashi, T. Shirai, E. Fluck, *Hyp. Int.* **46**, 725 (1989).
- [4] H. Inoue, H. Iwase, S. Yanagisawa, *Inorg. Chim. Acta* **7**, 259 (1973).
- [5] D. B. Brown, *Inorg. Chem.* **14**, 2582 (1975).
- [6] J. Fernandez-Bertran, E. Reguera, *Spectrosc. Lett.* **28**, 1015 (1995).
- [7] A. N. Garg, P. S. Goel, *Inorg. Chem.* **10**, 1344 (1971).
- [8] E. Reguera, J. F. Bertran, J. Miranda, A. Dago, *Hyp. Inter.* **77**, 1 (1993).
- [9] H. Binder, *Z. Anorg. Allg. Chem.* **429**, 247 (1977).
- [10] S. Ganguli, M. Bhattacharya, *J. Chem. Soc. Faraday Trans. I* **79**, 1513 (1983).
- [11] H. Inoue, S. Yanagisawa, *J. Inorg. Nucl. Chem.* **36**, 1409 (1974).
- [12] B. E. Saltzman, *Anal. Chem.* **26**, 1949 (1954).
- [13] Y. Morioka, T. Hisamitsu, H. Inoue, N. Yoshioka, H. Tomizawa, E. Miki, *Bull. Chem. Soc. Jpn.* **71**, 837 (1998).
- [14] H. Inoue, N. Yoshioka, Y. Morioka, *Hyp. Inter. (C)* **3**, 113 (1998).